Journal of Inflammation Research

Dovepress
Taylor & Francis Group

Open Access Full Text Article

ORIGINAL RESEARCH

Bioinformatic Analysis and Experimental Verification Reveal the Protective Role of Baicalein Against LPS-Induced Endothelial Cell Dysfunction

Fuping Luo*, Jinxi Ao*, Yuan Chen, Yan Cui, Xianghai Gan, Mengqin Li

Department of Emergency Medicine, Affiliated Hospital of North Sichuan Medical College, Nanchong, Sichuan, 637000, People's Republic of China

*These authors contributed equally to this work

Correspondence: Mengqin Li, Email limengqinfeifei@163.com

Background: Endothelial cells play a central role in the pathogenesis of sepsis. Currently, effective therapeutic options for sepsis remain limited. Baicalein (BAI) is a compound with multiple bioactivities. This study aims to investigate the protective effects of BAI against lipopolysaccharide (LPS)-induced endothelial cell injury and to explore the underlying molecular mechanisms.

Methods: Bioinformatics tools, including RNA sequencing (RNA-seq), immune cell infiltration analysis, Gene Ontology (GO) and Kyoto Encyclopedia of Genes and Genomes (KEGG) pathway enrichment analyses, were utilized to explore the molecular mechanisms of BAI in human umbilical vein endothelial cells (HUVECs) induced by LPS. The LPS-induced HUVECs model was used to assess the effects of BAI through CCK8 assays, cell permeability assays, and RT-qPCR.

Results: RNA-seq analysis revealed a set of differentially expressed genes (DEGs) shared between the Control group vs LPS group and LPS vs Baicalein group, including vascular cell adhesion molecule 1 (VCAM1), phosphoinositide-specific phospholipase C X-domain containing 1 (PLCXD1), and MIR3142 host gene (MIR3142HG), a long non-coding RNA. GO, KEGG, and Reactome enrichment analyses indicated that the DEGs were primarily enriched in TNF signaling, NF-κB signaling, and immune regulation pathways. Molecular docking and molecular dynamics simulation analyses revealed that BAI exhibits a strong binding affinity for key targets VCAM1 and PLCXD1. ROC analysis revealed that these core genes, VCAM1 and PLCXD1, exhibited significant diagnostic potential for sepsis. The cell experimental results demonstrated that BAI significantly alleviated the expression levels of inflammatory markers (such as IL-6 and IL-1β) and reduced endothelial cell permeability induced by LPS in HUVECs.

Conclusion: BAI may alleviate LPS-induced endothelial cell injury by modulating the inflammatory response and immune microenvironment through the regulation of MIR3142HG, VCAM1, and PLCXD1 targets. This study provides new molecular targets and theoretical insights for sepsis therapy.

Keywords: sepsis, Baicalein, endothelial cells, molecular mechanisms, biomarkers

Introduction

Sepsis is a systemic inflammatory response syndrome triggered by infection, often accompanied by multiple organ dysfunction, posing a significant threat to patients' lives.[1] Endothelial cell dysfunction plays a central role in the pathophysiology of sepsis. Increased permeability and disruption of the endothelial barrier can lead to tissue edema, microcirculatory disturbances, and multiple organ failure.[2] Endothelial cells serve as a bridge between local and systemic immune responses. During the progression of sepsis, bacterial components activate endothelial cells, leading to the production of inflammatory mediators such as IL-1β, IL-6, and TNF-α.[3] Gram-negative bacterial infection is one of the primary triggers of sepsis. Its cell wall component, lipopolysaccharide (LPS), serves as a key pathogen-associated molecular pattern (PAMP). LPS is densely distributed on the bacterial surface during the exponential growth phase, with approximately 2×10^6 LPS molecules covering 75% of the bacterial surface area.[4] LPS is a crucial factor in inducing endothelial cell injury associated with sepsis.[5] LPS induces the TLR4-dependent signaling pathway by binding to the CD14/TLR4/MD-2 receptor complex, activating both MyD88-dependent and -independent

https://doi.org/10.2147/JIR.S555260
Received: 21 July 2025
Accepted: 24 January 2026
Published: 27 February 2026

pathways, and ultimately triggering the activation of transcription factors such as NF-κB and MAPK. This leads to increased expression of pro-inflammatory cytokines and adhesion molecules.[6–9] Therefore, targeting the mechanisms of LPS-induced endothelial cell damage is of significant clinical importance for the prevention and treatment of sepsis.

Baicalein (BAI), a flavonoid compound extracted from the traditional Chinese medicine Scutellaria baicalensis, exhibits various biological activities, including anti-inflammatory, antioxidant, and anti-apoptotic effects.[10–12] Studies have shown that BAI can alleviate endothelial cell pyroptosis by inhibiting the NLRP3/Caspase-1/Gasdermin D pathway,[13] and it has demonstrated endothelial protective effects in various disease models.[14,15] However, the specific molecular mechanisms by which BAI modulates endothelial cell injury in sepsis have not been fully elucidated. In recent years, the development of RNA sequencing (RNA-seq) and bioinformatics analysis techniques has provided powerful tools for systematically identifying key drug targets and signaling pathways.

This study aims to explore the protective effects of BAI on LPS-induced injury in human umbilical vein endothelial cells (HUVECs) using RNA-seq technology and various bioinformatics approaches. This research provides new experimental evidence for the endothelial protective effects of BAI and offers potential molecular targets and theoretical support for the diagnosis and treatment of sepsis.

Materials and Methods

Cell Culture

HUVECs were purchased from ScienCell Research Laboratories, Inc. (USA) and cultured in a 5% CO_2, 37°C incubator. The cells were cultured in Endothelial Cell Medium (Catalog#1001, ECM; ScienCell), supplemented with 5% fetal bovine serum (FBS), 1% Endothelial Cell Growth Supplement (ECGS), and 1% antibiotics (penicillin/streptomycin). All experimental materials were sterilized using X-ray irradiation (SHARP 50, Raycision Medical Technology Co., Ltd) prior to use. The cells were divided into three groups: the Control group treated with PBS, the LPS group treated with 5 μg/mL LPS (L2630, Sigma) for 24 hours, and the Baicalein group treated with 5 μg/mL LPS and 10 μM Baicalein (BAI; Chengdu Mantsite Biotechnology Co., Ltd.) for 24 hours.

RNA Sequencing and Data Analysis

Total RNA was extracted from HUVECs in the Control, LPS, and Baicalein groups. RNA concentration and purity were assessed using a Nanodrop2000, integrity was evaluated by agarose gel electrophoresis, and the RNA Quality Number (RQN) was determined using the Agilent 5300. RNA quantity was required to be ≥1 μg, with a concentration ≥30 ng/μL and RQN >6.5, and the OD260/280 ratio between 1.8–2.2. mRNA was isolated using Oligo(dT) magnetic beads and fragmented to 300 bp using fragmentation buffer. Reverse transcription was performed to synthesize cDNA, followed by end repair, A-tail addition, adapter ligation, purification, size selection, and PCR amplification to construct the library. The library was quantified using Qubit 4.0, pooled, and loaded for sequencing. Clusters were generated by bridge PCR on the cBot platform, and sequencing was performed. Differentially expressed genes between the Control, LPS, and Baicalein groups were identified using DESeq2, with a threshold of $|\log2FC| \geq 1$ and padjust < 0.05.

Functional Enrichment Analysis

Gene Ontology (GO), Kyoto Encyclopedia of Genes and Genomes (KEGG), Reactome, and Disease Ontology (DO) enrichment analyses were performed using the "Majorbio" platform (https://cloud.majorbio.com/page/project/overview). The biological processes (BP), cellular components (CC), molecular functions (MF), signaling pathways, and disease associations related to the intersecting targets were analyzed.

Datasets

Microarray datasets GSE28750 and GSE134347 were retrieved from the Gene Expression Omnibus (GEO; https://www.ncbi.nlm.nih.gov/geo/). The GSE28750 dataset includes 41 samples: 10 from sepsis patients and 20 from controls. The GSE134347 dataset includes 298 samples: 156 from sepsis patients and 83 from controls.

Molecular Docking

The binding affinity of VCAM1 and PLCXD1 core targets with Baicalein was verified using molecular docking. The 3D structures of the targets were downloaded from the RCSB Protein Data Bank (https://www.rcsb.org/). The 2D structure files of the active compounds were retrieved from PubChem (SDF format). AutoDockTools 1.5.6 was used to process the protein targets and small molecules, and molecular docking was performed using Vina 1.5.6. Visualization was carried out using PyMOL.

Molecular Dynamics Simulation

This study conducted molecular dynamics simulation using the Gromacs 2022 software platform. The force field parameters for the protein system were obtained via the pdb2gmx tool and the AutoFF network platform, with the receptor protein modeled using the CHARMM36 force field and the ligand molecule using the CGenff force field parameters. During system construction, a cubic water box with a 1 nm edge was used for solvation, employing the TIP3P water model. The appropriate ions were added using the gmx genion tool to maintain system electroneutrality.For simulation parameters, long-range electrostatic interactions were treated using the PME (Particle Mesh Ewald) method with a cutoff radius of 1 nm. The SHAKE algorithm was applied to constrain all chemical bonds, and the Verlet leapfrog algorithm with a 1 fs time step was used for the dynamics calculations. Before the official simulation, the system underwent energy minimization in a three-stage process: 1) solute was fixed, and water molecules were optimized; 2) counter-ions were fixed, and the system was optimized; 3) the entire system was optimized without constraints. The simulation was run for 100 ns under constant temperature (310 K) and pressure (NPT).Standard GROMACS analysis tools were used to calculate various structural parameters: g-rmsd to analyze root-mean-square deviation (RMSD), g-rmsf to assess root-mean-square fluctuation (RMSF), g-hbond to count hydrogen bonds (HBonds), g-Rg to determine radius of gyration (Rg), and g-sasa to calculate solvent-accessible surface area (SASA). Additionally, MM-PBSA binding free energy calculations were performed using the g_mmpbsa module.

Receiver Operating Characteristic (ROC) Curve

ROC curves were generated using the "pROC" package based on datasets GSE28750 and GSE134347 to evaluate the diagnostic value of VCAM1 and PLCXD1 in sepsis patients.

Nomogram Diagram

Based on high-throughput sequencing data, differential expression analysis was performed to identify potential core genes associated with sepsis. The diagnostic value of these genes was assessed using multivariate logistic regression analysis, and a nomogram model for diagnosis was constructed using the rms package in R. A calibration curve was used to evaluate the performance of the nomogram.

Immune Cell Infiltration Analysis

Immune cell infiltration analysis was performed using the CIBERSORT algorithm on the GSE28750 and GSE134347 datasets. The proportions of 22 immune cell types in each sample were calculated. The Wilcoxon test was used to compare the differences in immune cell infiltration levels between the sepsis and control groups. Subsequently, Pearson correlation analysis was applied to examine the correlation between VCAM1 and PLCXD1 gene expression and the different immune cells.

Cell Viability Assay

HUVECs were treated with various concentrations of BAI (0, 5, 10, 20, 40, 60, 80, 100, 200 μmol/L) for 24 hours, and cell viability was assessed using the CCK-8 assay. Cells were seeded at 5000 per well in 96-well plates, with a final volume of 100 μL per well. After 24 hours of incubation at 37°C, 5% CO_2, 10 μL of CCK-8 solution (AG51006, Aikerui Biotech) was added to each well, and cells were incubated for 1 hour. Absorbance at 450 nm was measured.

In vitro Permeability Assay

HUVECs were seeded into Transwell-24 chambers (Corning, New York, USA) and grouped based on experimental requirements. After cell adhesion, the chamber contents were aspirated, washed three times with PBS, and incubated with FITC-Dextran for 1 h at 37°C. Samples were then collected from the upper and lower chambers. The dextran permeability coefficient (Pd), reflecting HUVECs permeability, was calculated using the formula: $Pd = [A]/t \times 1/A \times V/[L]$, where [A] is the absorbance of the lower chamber, t is the time in seconds, A is the membrane area (cm^2), V is Volume of liquid in the lower chamber, and [L] is the absorbance of the upper chamber (fluorescence intensity).

RT-qPCR

RT-qPCR was performed on a Bio-Rad CFX96 instrument with the following reaction mixture: 10 μL ChamQ SYBR Color qPCR Master Mix, 0.4 μL of each forward and reverse primer, 2 μL cDNA template, and 7.2 μL ddH_2O. The PCR cycling conditions were: 95°C for 30 sec; 95°C for 10 sec, 60°C for 30 sec for 40 cycles, followed by a melting curve analysis. The PCR primer sequences are listed in Table 1.

Statistical Analysis

The experimental data in this study are presented as mean ± standard deviation (SD). Comparisons between two groups were performed using the *t*-test, while comparisons among more than two groups were conducted using one-way analysis of variance (ANOVA). Statistical analysis was performed using GraphPad Prism 10.0. A p-value of < 0.05 was considered statistically significant.

Results

Identification of Differentially Expressed Genes

A total of 32,815 expressed genes and 151,658 expressed transcripts were detected in this analysis. In the comparison between the Control and LPS groups, 359 DEGs were identified, with 313 genes being upregulated and 46 downregulated. In the comparison between the LPS and Baicalein groups, 57 DEGs were detected, with 26 upregulated and 31 downregulated (Figure 1A–F). The intersection of DEGs between the Control and LPS groups and between the LPS and Baicalein groups revealed three common genes: vascular cell adhesion molecule 1 (VCAM1), phosphatidylinositol specific phospholipase C X domain containing 1 (PLCXD1), and MIR3142HG (Figure 1G).

Functional Enrichment Analysis of Differentially Expressed Genes

The molecular mechanisms underlying the effects of BAI on biological processes, cellular components, and molecular functions on LPS-induced endothelial cell damage were investigated. GO enrichment analysis was performed on DEGs from the Control and LPS groups, as well as the LPS and Baicalein groups (Figure 2A and B). The DEGs from the Control and LPS groups were significantly enriched in 1,519 GO terms related to biological processes, 138 GO terms related to cellular components, and 272 GO terms related to molecular functions. The DEGs from the LPS and Baicalein groups were significantly enriched in 435 GO terms related to biological processes, 23 GO terms related to cellular components, and 78 GO terms related to molecular functions. Among the top 20 biological process GO terms that were significantly enriched in the DEGs of both the Control vs LPS and LPS vs Baicalein comparisons, many were closely associated with inflammatory responses. Additionally, KEGG pathway enrichment analysis of the DEGs was conducted

Table 1 PCR Primer Sequences

Genes	Primer Sequences
IL-6	FCTGCAAGAGACTTCCATCCAGRTCGCTCCTGGAAGATGGTGAT
IL-1β	FGAAATGCCACCTTTTGACAGTRTGGATGCTCTCATCAGGACAG
GAPDH	FCAGTGGCAAAGTGGAGATTGTTGR AGTGGTATAGACAGGTCTGTTG

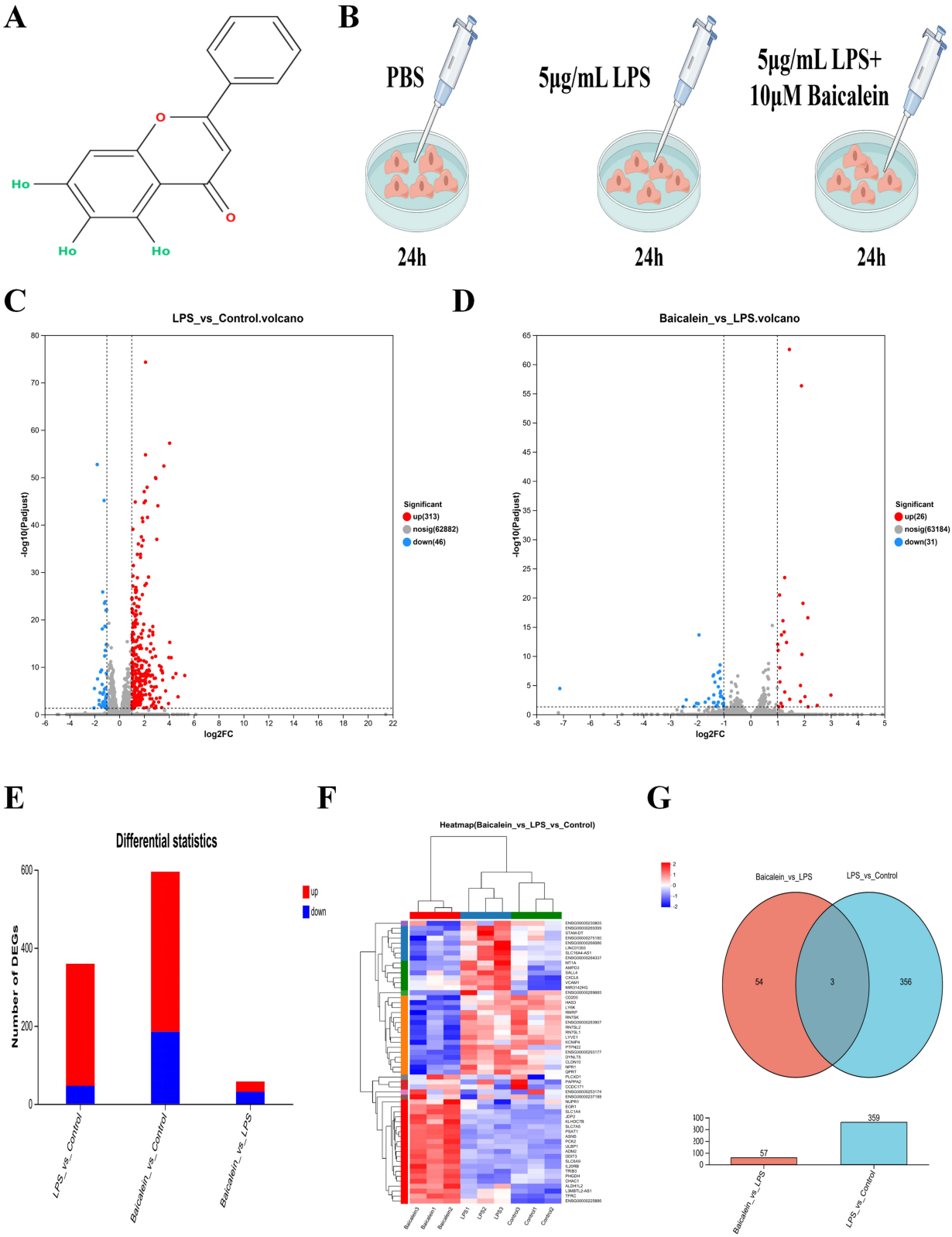

Figure 1 DEGs in LPS-Induced HUVECs Treated with BAI. (**A**) Chemical structure of BAI. (**B**) Experimental scheme for treating LPS-induced HUVECs with BAI. (**C**) Volcano plot of DEGs between the Control and LPS groups. (**D**) Volcano plot of DEGs between the Baicalein and LPS groups. (**E**) Stacked plot of DEGs between the Control and LPS groups, as well as between the Baicalein and LPS groups. (**F**) Heatmap of DEGs in the Control, LPS, and Baicalein groups. (**G**) Venn diagram showing the intersection of DEGs between the Control and LPS groups, as well as between the LPS and Baicalein groups.

https://doi.org/10.2147/JIR.S555260

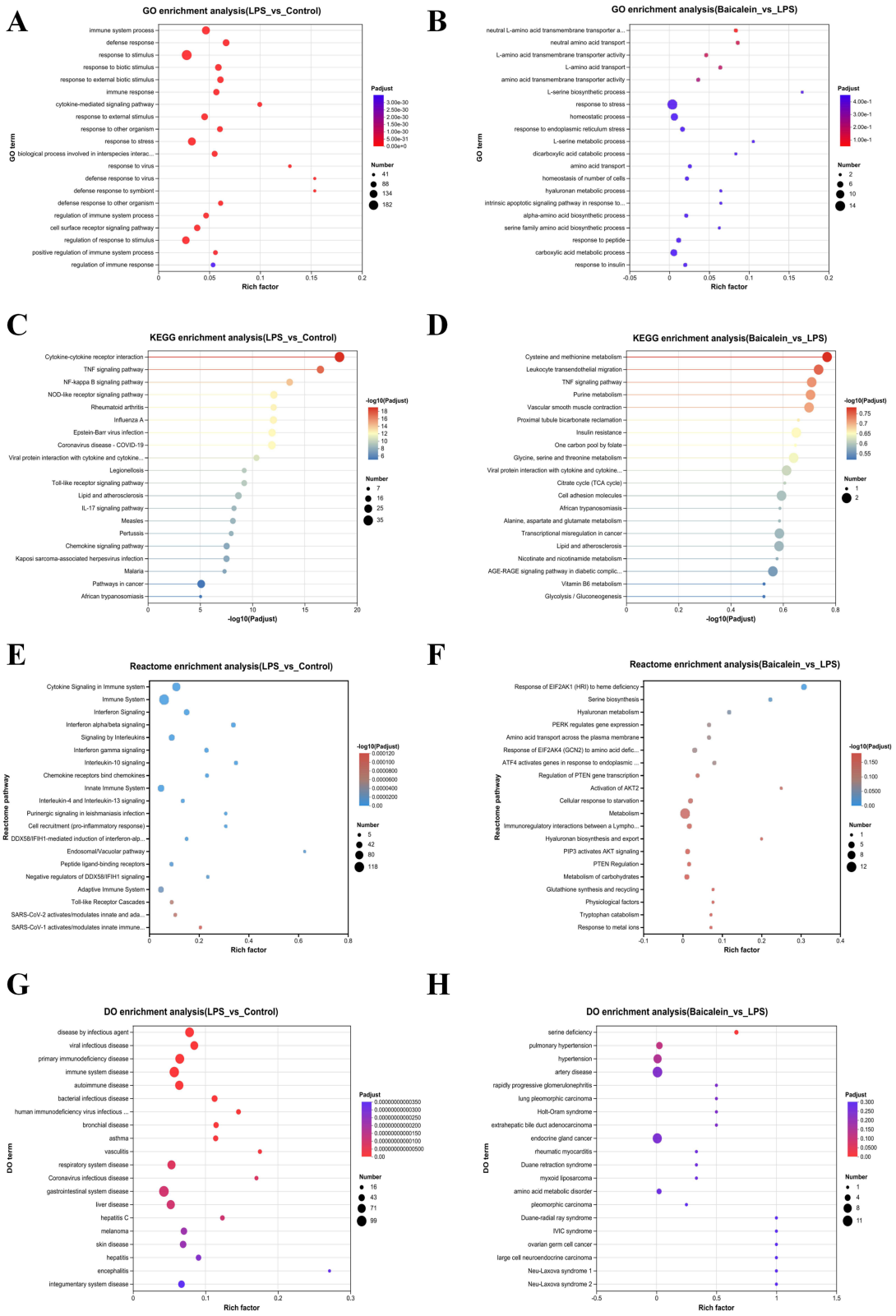

Figure 2 Enrichment Analysis of DEGs in LPS-Induced HUVECs Treated with BAI. (**A**) GO enrichment analysis of DEGs between the Control and LPS groups. (**B**) GO enrichment analysis of DEGs between the Baicalein and LPS groups. (**C**) KEGG pathway enrichment analysis of DEGs between the Control and LPS groups. (**D**) KEGG pathway enrichment analysis of DEGs between the Baicalein and LPS groups. (**E**) Reactome enrichment analysis of DEGs between the Control and LPS groups. (**F**) Reactome enrichment analysis of DEGs between the Baicalein and LPS groups. (**G**) DO enrichment analysis of DEGs between the Control and LPS groups. (**H**) DO enrichment analysis of DEGs between the Baicalein and LPS groups.

https://doi.org/10.2147/JIR.S555260

(Figure 2C and D). The DEGs from the Control and LPS groups showed significant enrichment in the TNF signaling pathway, NF-κB signaling pathway, NOD-like receptor signaling pathway, Toll-like receptor signaling pathway, and IL-17 signaling pathway. The DEGs from the LPS and Baicalein groups was highly enriched in pathways related to cysteine and methionine metabolism, leukocyte transendothelial migration, and the TNF signaling pathway. The differential gene VCAM1 was co-enriched in the TNF signaling pathway across both the Control vs LPS and LPS vs Baicalein comparisons. Reactome enrichment analysis revealed that the DEGs from the Control and LPS groups primarily involved immune and inflammatory response pathways, while the LPS and Baicalein groups primarily involved metabolic and stress response pathways. BAI may exert its effects by modulating metabolic and stress response pathways, which in turn could influence LPS-induced immune and inflammatory responses (Figure 2E and F). DO enrichment analysis identified diseases significantly associated with these genes (Figure 2G and H). The DEGs from the Control and LPS groups were mainly associated with diseases related to the immune system, infections, and the respiratory system. In contrast, the DEGs from the LPS and Baicalein groups were primarily linked to diseases related to metabolism, cancer, and genetic disorders.

Identification and Validation of Intersection Genes

Molecular docking was used to assess the binding affinity between the intersection genes and BAI. The results showed that the intersection target MIR3142HG, a long non-coding RNA (lncRNA), could not be docked. For the remaining intersection targets, VCAM1 and PLCXD1, molecular docking was conducted. Both VCAM1 and PLCXD1 exhibited binding energies with BAI greater than −5.0 kcal·mol^{-1}, suggesting a favorable binding interaction between BAI and these two proteins (Figure 3A–C). Further, molecular dynamics simulation were employed to verify the binding affinity

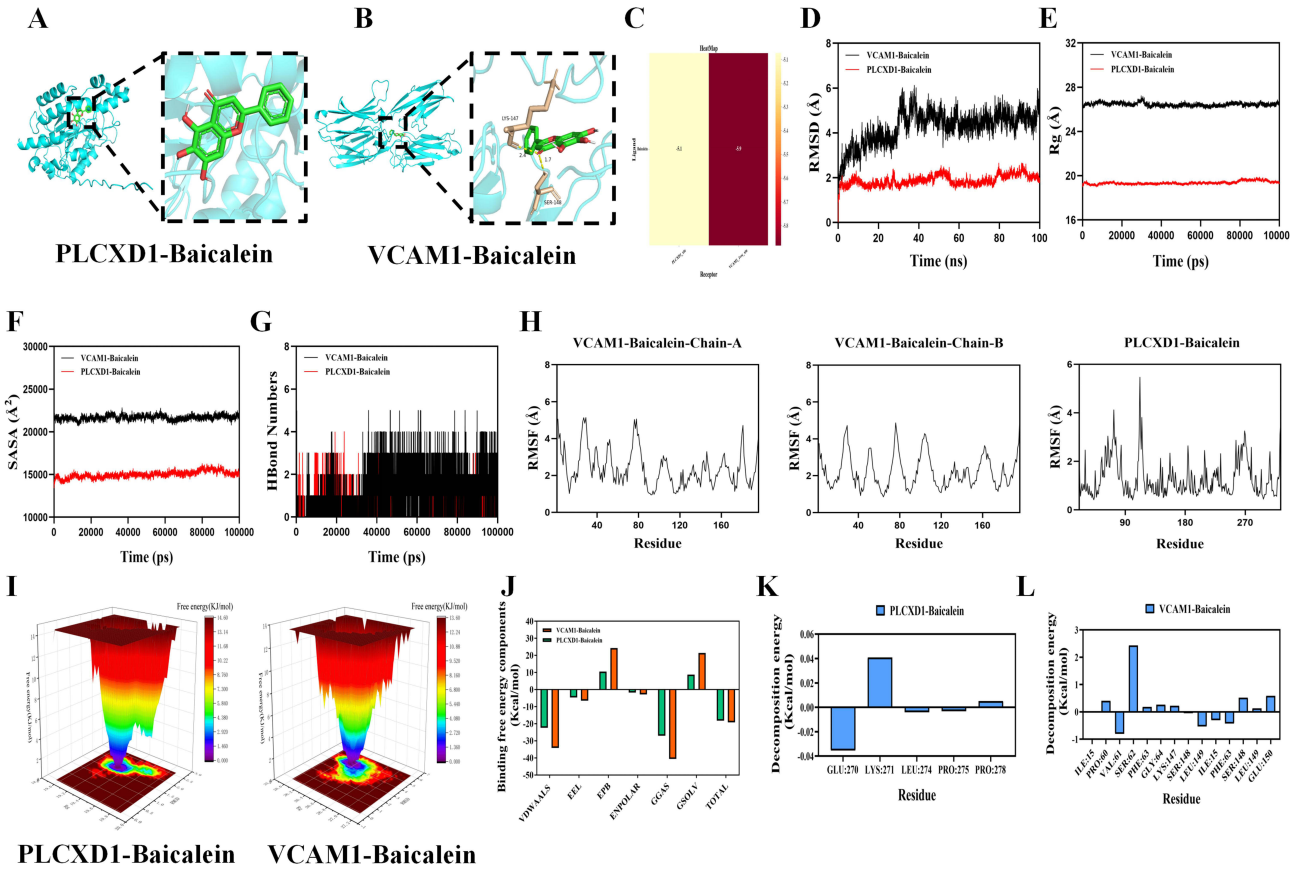

Figure 3 Identification and validation of common genes in LPS-induced HUVECs treated with BAI.(**A**) Molecular docking of PLCXD1 with BAI.(**B**) Molecular docking of VCAM1 with BAI.(**C**) Binding energy of VCAM1 and PLCXD1 with BAI.(**D**) RMSD values of the protein-ligand complex over time.(**E**) Rg values of the protein-ligand complex over time.(**F**) SASA values of the protein-ligand complex over time.(**G**) HBonds values of the protein-ligand complex over time.(**H**) RMSF values of the protein-ligand complex.(**I**) Free energy landscape.(**J-L**) MMPBSA binding free energy calculation.

https://doi.org/10.2147/JIR.S555260

of VCAM1 and PLCXD1 with BAI (Figure 3D–L).Root Mean Square Deviation (RMSD) analysis was used to evaluate the conformational stability of the protein-ligand complexes. This metric reflects the deviation of atomic positions relative to the initial structure, with lower RMSD values indicating greater stability. The VCAM1-Baicalein complex reached dynamic equilibrium after 50 ns (RMSD ≈ 5.3 Å), while the PLCXD1-Baicalein system stabilized after 60 ns (RMSD ≈ 1.9 Å), demonstrating the formation of stable complexes between baicalein and both target proteins. Radius of Gyration (Rg) analysis revealed that the Rg values of both complexes remained relatively constant, suggesting no significant structural expansion or contraction during the simulation. Solvent Accessible Surface Area (SASA) analysis further confirmed that ligand binding did not significantly alter the protein surface accessibility, indicating minimal impact on the overall protein conformation.Hydrogen bonding analysis showed that the VCAM1-Baicalein complex maintained an average of three hydrogen bonds (range: 0–5), while the PLCXD1-Baicalein system had an average of two hydrogen bonds (range: 0–4), confirming stable intermolecular interactions between the ligand and target proteins. Root Mean Square Fluctuation (RMSF) analysis indicated that the flexibility of amino acid residues in both complexes was low (RMSF < 4 Å), further supporting the conformational stability of the systems.Free Energy Landscape (FEL) analysis based on RMSD and Rg demonstrated the conformational distribution of the complexes, with the energy gradient (red → blue) clearly illustrating the energy landscape. MM/PBSA binding free energy calculations revealed significant binding affinity for both complexes, with VCAM1-Baicalein (ΔG = −19.17 kcal/mol) and PLCXD1-Baicalein (ΔG = −18.24 kcal/mol). The VCAM1 complex showed a stronger binding tendency. Key residue energy decomposition analysis identified GLU270, LEU274, and PRO275 in the PLCXD1 system, as well as VAL61, LEU149, PHE63, and ILE15 in the VCAM1 system, as significantly contributing to the binding free energy, suggesting these residues play a crucial role in the molecular recognition process. In summary, baicalein forms stable complexes with both VCAM1 and PLCXD1, with specific hydrogen bond networks and interactions with key amino acid residues involved in the binding process. This study primarily focuses on the regulatory network of baicalein on protein-coding genes, thus MIR3142HG was not included in subsequent experimental verification.Based on the GSE28750 and GSE13434 datasets, violin plots were generated, showing that VCAM1 expression was significantly elevated in sepsis patients, while PLCXD1 expression was notably reduced. These results align with those observed in our study's Control and LPS groups. After baicalein intervention, VCAM1 expression significantly decreased, and PLCXD1 expression increased (Figure 4A and B).ROC curve analysis of VCAM1 and PLCXD1 based on the GSE28750 and GSE13434 datasets was conducted to assess their diagnostic value in sepsis. The area under the curve (AUC) for both genes exceeded 0.6, suggesting that these core genes hold diagnostic reference value in sepsis differentiation (Figure 4C and D). Furthermore, a nomogram model based on these two biomarkers was developed (Figure 4E and F), with an AUC greater than 0.7, and decision curve analysis indicated that this nomogram model provides significant clinical benefit.

Immune Cell Infiltration Analysis of Intersection Genes

The CIBERSORT algorithm was used to calculate the immune cell infiltration abundance of 22 immune cell types in sepsis. Wilcoxon tests were then performed to compare the differences in immune cell infiltration levels between the sepsis and normal groups. The results revealed that neutrophils, macrophages M0, monocytes, mast cells activated, and macrophages M1 were significantly increased in the sepsis group, while T cells CD4+ naive, NK cells resting, B cells memory, and dendritic cells activated were significantly decreased (Figure 5A–C) (Table S1). To explore the association between the common genes VCAM1 and PLCXD1 and immune cells in sepsis, Pearson correlation coefficients were calculated between these genes and different immune cell types. The results indicated significant correlations: VCAM1 was positively correlated with plasma cells and macrophages M0, and negatively correlated with T cells CD4+ resting memory, and B cells memory. PLCXD1 was positively correlated with T cells CD8+ and NK cells resting, and negatively correlated with neutrophils and γδ T cells (Figure 5D). These findings suggest that VCAM1 and PLCXD1 may play significant roles in the immune microenvironment of sepsis.

Functional Enrichment of Intersection Genes

GO enrichment analysis of the intersection Genes revealed that they are primarily associated with immune cell adhesion, migration, inflammation, angiogenesis, calcium signaling, and interferon signaling pathways (Figure 6A). KEGG

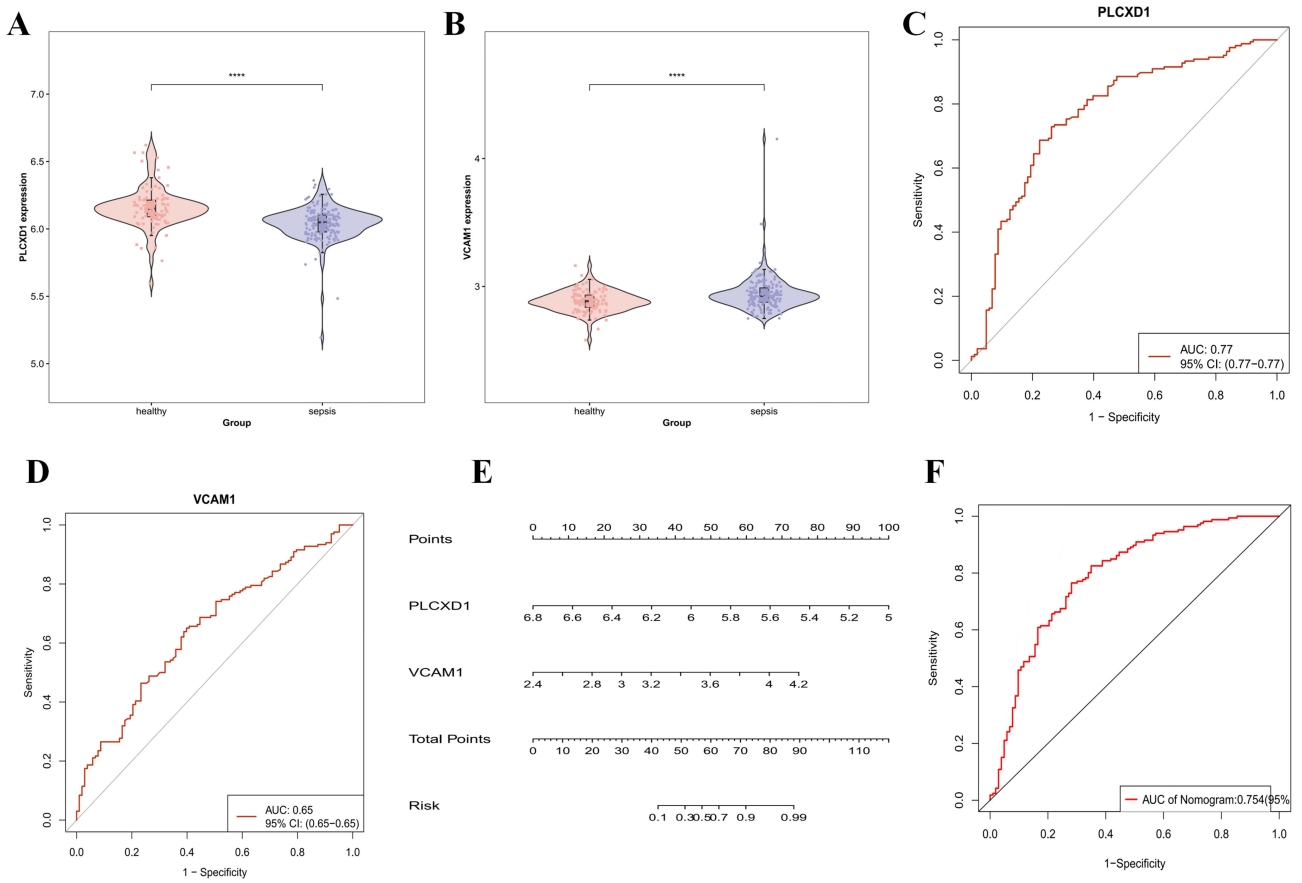

Figure 4 Identification and Validation of Intersection Genes in LPS-Induced HUVECs Treated with BAI.(**A**) Violin plot of PLCXD1 expression.(**B**) Violin plot of VCAM1 expression.(**C**) ROC curve of PLCXD1.(**D**) ROC curve of VCAM1.(**E**) Nomogram for VCAM1 and PLCXD1.(**F**) ROC curve of the nomogram for VCAM1 and PLCXD1. ****P < 0.0001.

pathway analysis showed significant enrichment in the TNF signaling pathway and NF-κB signaling pathway (Figure 6B). Reactome analysis indicated enrichment in IL-4 and IL-13 signaling, TNF signaling, interleukin signaling, and cytokine signaling in the immune system (Figure 6C). DO enrichment analysis revealed that the common genes are associated with immune-related diseases, such as rheumatic myocarditis and lupus nephritis, and infectious diseases, including dengue and viral encephalitis (Figure 6D). These results suggest that these three common genes play crucial roles in immune regulation and infection responses, potentially serving as important targets for future studies on immune-related diseases.

BAI Alleviates LPS-Induced HUVECs Damage

CCK8 assays were performed to assess the effect of BAI on endothelial cell viability. The results showed that BAI at concentrations ranging from 0 to 200 μmol/L did not significantly affect HUVECs viability ($P > 0.05$) (Figure 7A), and 10 μmol/L was selected for subsequent experiments. Compared to the Control group, LPS intervention significantly increased HUVECs permeability ($P < 0.05$), while BAI treatment significantly reduced HUVECs permeability ($P < 0.05$). Inflammatory cytokines are important markers of HUVECs damage (Figure 7B and C). Compared to the Control group, the LPS group exhibited significantly elevated levels of IL-6 and IL-1β in HUVECs ($P < 0.05$); however, BAI treatment significantly reduced IL-6 and IL-1β levels ($P < 0.05$) (Figure 7D and E).

Discussion

Sepsis is characterized by high morbidity and mortality rates.[16,17] Among the complex pathophysiological mechanisms of sepsis, endothelial cells play a central role in regulating microcirculation and maintaining the vascular barrier.

https://doi.org/10.2147/JIR.S555260

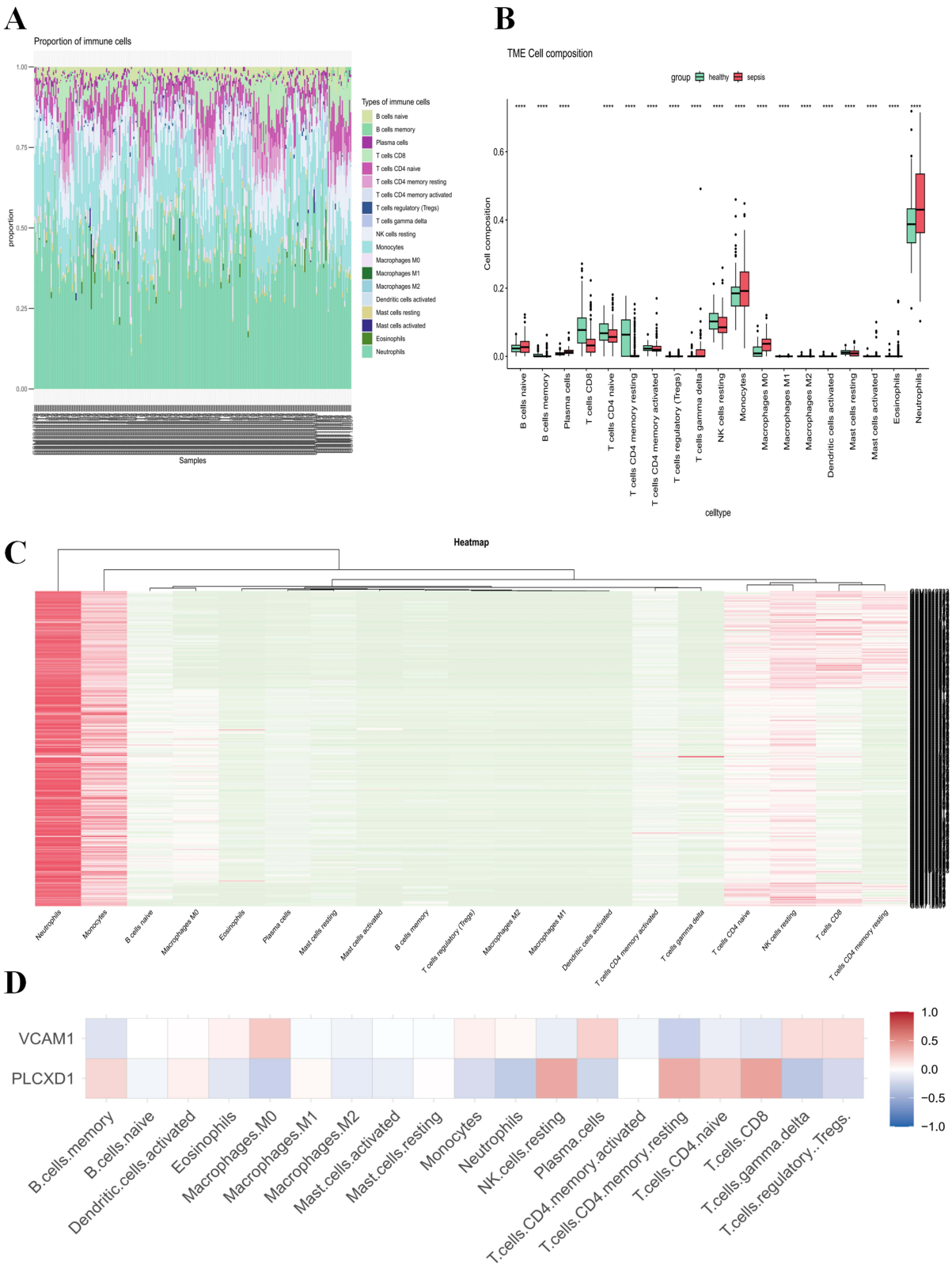

Figure 5 Immune Cell Infiltration of Intersection Genes in LPS-Induced HUVECs Treated with BAI.(**A**) Bar plot showing the proportion of 22 immune cell types in each sample.(**B**) Box plot illustrating the proportions of 22 immune cell types between the Control and Sepsis groups.(**C**) Heatmap depicting the distribution of 22 immune cell types between the Control and Sepsis groups.(**D**) Correlation between the expression levels of VCAM1 and PLCXD1 with immune cell infiltration. ****P < 0.0001.

https://doi.org/10.2147/JIR.S555260

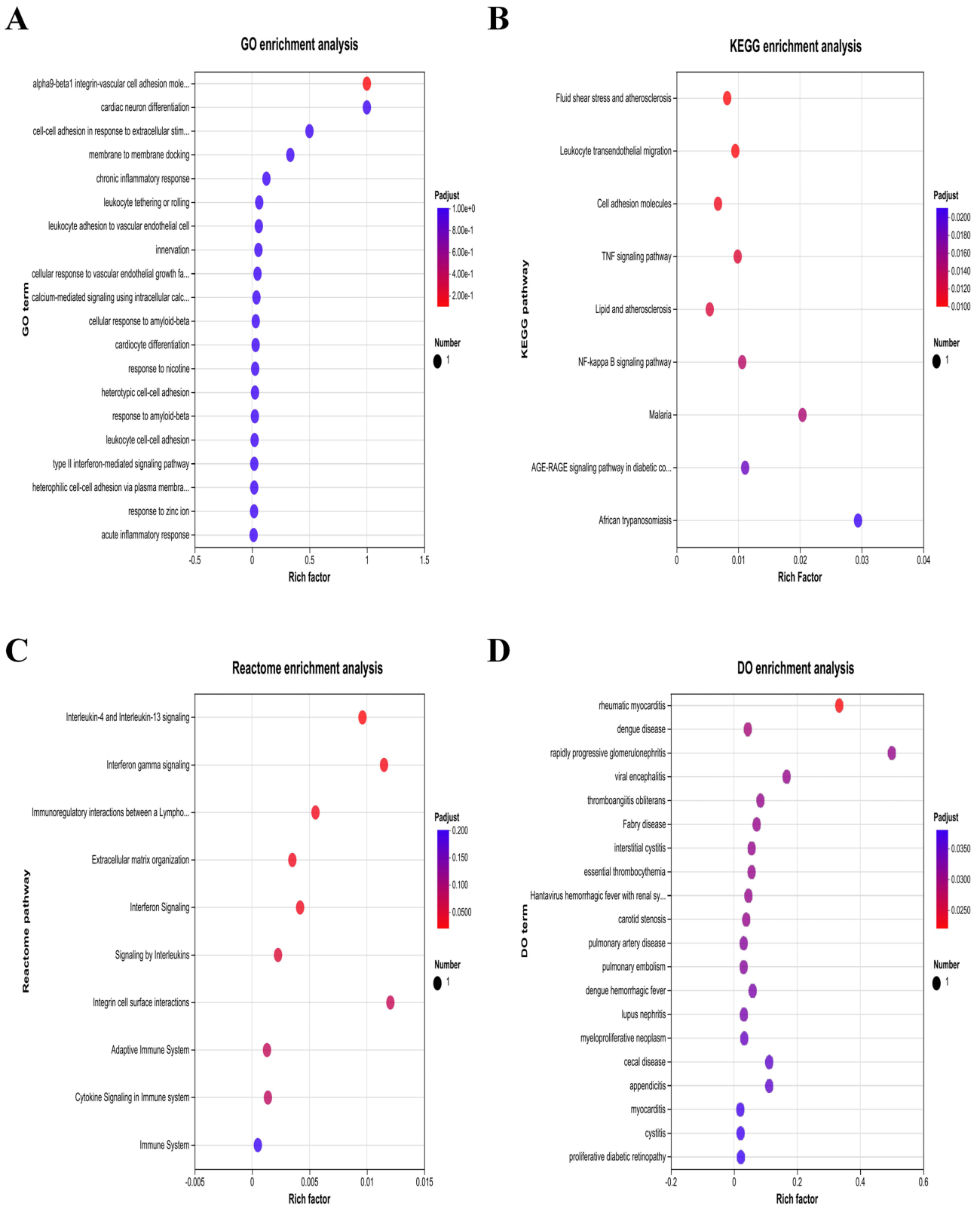

Figure 6 Functional Enrichment Analysis of the Intersection Genes in BAI-treated LPS-induced HUVECs. (**A**) GO Enrichment Analysis of the intersection Genes. (**B**) KEGG Pathway Enrichment Analysis of the intersection Genes. (**C**) Reactome Enrichment Analysis of the intersection Genes. (**D**) DO Enrichment Analysis of the intersection Genes.

https://doi.org/10.2147/JIR.S555260

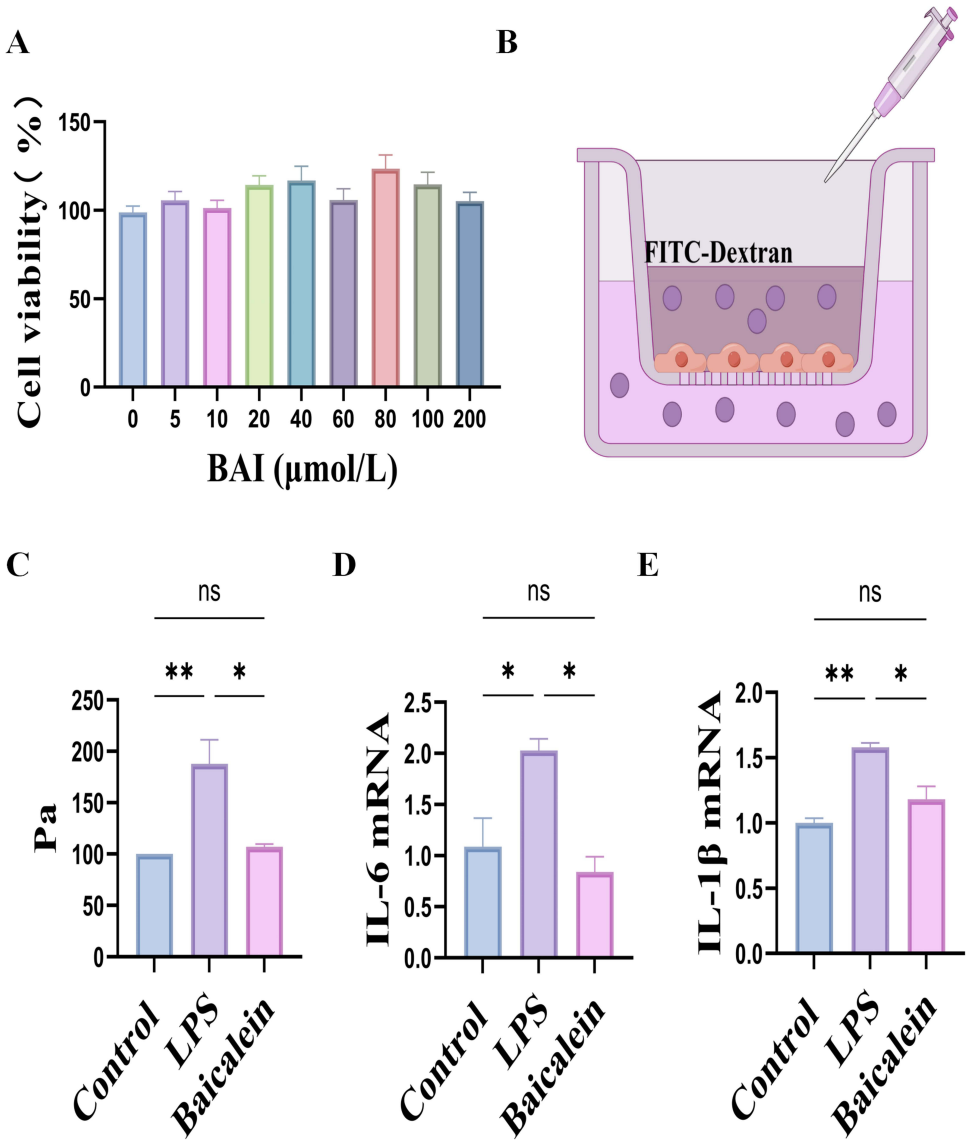

Figure 7 BAI Alleviates LPS-Induced Cell Damage in HUVECs. (**A**) Effect of different concentrations of BAI on HUVECs viability (n = 6). (**B**) Schematic diagram of the HUVECs in vitro permeability assay. (**C**) Statistical analysis of the HUVECs in vitro permeability assay (n = 3). (**D**) RT-qPCR analysis of IL-6 mRNA expression levels in HUVECs (n = 3). (**E**) RT-qPCR analysis of IL-1β mRNA expression levels in HUVECs (n = 3). *P < 0.05, **P < 0.01, ns: P > 0.05.

Endothelial dysfunction is a key factor leading to multiple organ injury.[18] However, an early diagnostic system for sepsis based on endothelial damage-specific biomarkers has yet to be established, and there is a lack of precision therapeutic strategies targeting endothelial protection. Baicalein, a traditional Chinese herbal compound, has been shown to inhibit the expression of the chemokine P-selectin in endothelial cell, thereby protecting them.[12] This study integrates RNA-seq transcriptomic sequencing, bioinformatics analysis, and experimental validation to explore the protective effects of BAI on lipopolysaccharide (LPS)-induced HUVECs damage and its underlying molecular mechanisms.

This study identified three potential genes—MIR3142HG, VCAM1, and PLCXD1—by intersecting the differentially expressed genes from the Control and LPS groups, as well as the LPS and Baicalein groups. The long non-coding RNA (lncRNA) MIR3142HG, located at the 5q33.3 locus, is significantly upregulated in sepsis-induced acute lung injury (ALI).[19] Further mechanistic studies suggest that MIR3142HG promotes apoptosis and exacerbates the inflammatory response by regulating the miR-95-5p/JAK2 signaling axis, thus accelerating the progression of sepsis-induced ALI.[20] Moreover, MIR3142HG mediates LPS-induced damage in human pulmonary microvascular endothelial cell (HPMECs) via targeting miR-450b-5p/HMGB1, which mitigates LPS-induced ALI.[21] In our study, MIR3142HG expression was

elevated in the LPS group compared to the Control group, and its expression level was reduced following BAI intervention. VCAM-1, a significant member of the immunoglobulin superfamily,[22] is upregulated in sepsis models. Inhibition of hydrogen sulfide biosynthesis reduces the expression of VCAM-1 on endothelial cells of liver and lung tissues in cecal ligation and puncture (CLP)-induced sepsis, thereby decreasing leukocyte infiltration.[23] Pro-inflammatory cytokines, such as TNF-α, activate endothelial cell, which upregulate VCAM-1 on their surface. The activated VCAM-1 binds specifically to the α4β1 integrin (VLA-4) on leukocytes, further activating downstream signaling pathways, including ROC and calcium signaling.[22] Additionally, VCAM-1 enhances vascular permeability, promoting the extravasation of solutes and plasma, thus amplifying the inflammatory response in the microcirculation.[24] The sequencing results of this study indicate that, compared to the Control group, VCAM-1 expression was elevated in the LPS group, which is consistent with findings from the GSE28750 and GSE134347 datasets in septic patients. Additionally, ROC analysis suggests that VCAM-1 holds diagnostic value for sepsis.Following intervention with BAI, the expression of VCAM-1 was downregulated. Molecular docking and molecular dynamics simulation results indicated that BAI can spontaneously bind to VCAM-1.Phosphatidylinositol-specific phospholipase C X domain containing 1 (PLCXD1), located on the X and Y chromosomes, is a pseudogene with limited functional studies.[25] In human bladder carcinoma epithelial cell lines (EJ cells) treated with diallyl trisulfide (DATS), PLCXD1 expression was significantly upregulated.[26] A comparison between ischemic stroke patients and male controls revealed differential expression of PLCXD1 in the PAR region of the Y chromosome.[27] However, there is minimal research on the function of PLCXD1, particularly in the context of sepsis and endothelial cell. The sequencing results of this study revealed that, compared to the Control group, PLCXD1 expression was significantly reduced in the LPS group, consistent with findings from the GSE28750 and GSE134347 datasets of septic patients. Additionally, ROC analysis indicated that PLCXD1 possesses diagnostic value for sepsis. Following intervention with BAI, the expression of PLCXD1 was elevated. Molecular docking and molecular dynamics simulation results demonstrated that BAI can spontaneously bind to PLCXD1.

Endothelial cells are unconventional immune cells within the vasculature.[28] Neutrophils serve as the first line of defense against pathogens.[29] In infection or inflammation, activated neutrophils and their extracellular traps (NETs) exacerbate the pro-inflammatory and pro-angiogenic effects of endothelial cell, aggravating immune microenvironment imbalance.[30,31] Activated endothelial cells upregulate P-selectin, E-selectin, ICAM-1, and VCAM-1, promoting neutrophil recruitment and intensifying the inflammatory response.[32] In our study, immune infiltration analysis revealed a significant increase in neutrophils in septic patients, with PLCXD1 showing a significant negative correlation and VCAM-1 exhibiting a positive correlation with neutrophils, suggesting that endothelial cells may regulate neutrophil recruitment via VCAM-1 and PLCXD1, thereby improving the immune microenvironment. Macrophages, key effector cells of the innate immune system,[33] secrete pathogens that activate endothelial cell via Toll-like receptor-4 (TLR4) in sepsis, resulting in upregulated adhesion molecules, increased blood cell aggregation, and exacerbated inflammation and endothelial damage.[34,35] Modulating the expression of ICAM-1 and VCAM-1 on endothelial cell can influence macrophage infiltration in local tissues.[36] Our immune infiltration analysis showed a notable increase in M0 macrophages in septic patients, while M1 and M2 macrophages did not show significant elevation. This may be attributed to the rapid activation of macrophages during acute inflammation, yet their polarization is not complete; M0 macrophages, due to their high plasticity, rapidly respond to inflammatory stimuli. VCAM-1 was positively correlated with M0 macrophages, while PLCXD1 showed a negative correlation, suggesting that endothelial cell may regulate macrophages via VCAM-1 and PLCXD1, thereby improving the immune microenvironment.

This study employed functional and pathway enrichment analyses to investigate the core pathways and mechanisms underlying BAI's effects in treating LPS-induced endothelial cell damage. The results of differential expression analysis between the Control, LPS, and Baicalein groups, as well as the enrichment analysis of intersecting genes (VCAM1, PLCXD1, and MIR3142HG), highlighted the pivotal role of inflammation. KEGG enrichment analysis revealed significant activation of the TNF and NF-κB signaling pathways. Endothelial cells exhibit a bidirectional relationship with inflammation.[37] In sepsis, endotoxins like LPS activate the NF-κB and NLRP3 inflammasome pathways in endothelial cell, significantly upregulating pro-inflammatory cytokines and exacerbating endothelial damage, which contributes to systemic inflammation and multiple organ dysfunction syndrome (MODS).[38,39] Interleukins, such as IL-32, further exacerbate endothelial inflammation through the NF-κB pathway.[40] Sepsis-induced inflammatory responses

damage tight junction proteins, including ZO-1, compromising endothelial permeability.[41,42] This study demonstrates that in endothelial cell of the LPS-treated group, the expression of inflammatory cytokines IL-1β and IL-6 is upregulated, along with increased endothelial cell permeability. These abnormal expression patterns can be significantly ameliorated by intervention with BAI, suggesting that BAI plays a role in maintaining endothelial cell inflammatory responses and permeability induced by LPS.

Conclusions

This study systematically elucidates the mechanism by which BAI improves septic endothelial dysfunction through the regulation of key molecules such as VCAM1, PLCXD1, and MIR3142HG, based on multi-omics analysis and experimental validation. BAI was found to mitigate LPS-induced endothelial cell upregulation of MIR3142HG and VCAM1, as well as downregulation of PLCXD1. Furthermore, VCAM1 and PLCXD1 serve as early diagnostic markers for septic endothelial dysfunction. The close correlation between VCAM1, PLCXD1, and neutrophil and macrophage infiltration suggests their potential role as critical nodes linking endothelial injury with immune dysregulation. These findings not only provide novel diagnostic markers and therapeutic targets for septic endothelial injury but also lay a theoretical foundation for the clinical application of BAI. However, certain limitations exist in this study. For instance, MIR3142HG has not yet been further validated, and analyses at the level of animal models and clinical samples remain lacking. Future research should aim to investigate the dynamic changes of these molecules during the progression of sepsis and elucidate their precise regulatory mechanisms.

Ethics Approval and Consent to Participate

In accordance with Articles 32(1) and 32(2) of the "Measures for Ethical Review of Life Science and Medical Research Involving Human Subjects", issued on February 18, 2023, research may be exempt from ethical review under the following circumstances: (1) when utilizing legally obtained publicly available data, or data generated through observation of public behavior without interference; and (2) when conducting research using anonymized data. This study meets the criteria outlined in the aforementioned provisions, and therefore, is exempt from ethical review.

Consent for Publication

All authors approved the final version of the manuscript and Consent for publication.

Author Contributions

All authors made a significant contribution to the work reported, whether that is in the conception, study design, execution, acquisition of data, analysis and interpretation, or in all these areas; took part in drafting, revising or critically reviewing the article; gave final approval of the version to be published; have agreed on the journal to which the article has been submitted; and agree to be accountable for all aspects of the work.

Funding

This study was supported by the Nanchong Social Science Research "Fourteenth Five-Year Plan" 2024 Project [NC24B259].

Disclosure

The authors declare no competing interests in this work.

References

1. Y ZY, T NB. Signaling pathways and intervention therapies in sepsis. *Signal Transd Targeted Therapy*. 2021;6(1):407. doi:10.1038/s41392-021-00816-9
2. Fang Y, Li C, Shao R, et al. The role of biomarkers of endothelial activation in predicting morbidity and mortality in patients with severe sepsis and septic shock in intensive care: a prospective observational study. *Thrombosis Res*. 2018;171:149–154. doi:10.1016/j.thromres.2018.09.059
3. V DE, Wang K, Mandavilli R, et al. The effects of sepsis on endothelium and clinical implications. *Cardiovasc Res*. 2021;117(1):60–73. doi:10.1093/cvr/cvaa070

4. Klein G, Raina S. Regulated assembly of LPS, its structural alterations and cellular response to LPS defects. *Int J Mol Sci*. 2019;20(2):356. doi:10.3390/ijms20020356
5. Wang M, Feng J, Zhou D, et al. Bacterial lipopolysaccharide-induced endothelial activation and dysfunction: a new predictive and therapeutic paradigm for sepsis. *Eur J Med Res*. 2023;28(1):339. doi:10.1186/s40001-023-01301-5
6. Ciesielska A, Matyjek M, Kwiatkowska K. TLR4 and CD14 trafficking and its influence on LPS-induced pro-inflammatory signaling. *Cell Mol Life Sci*. 2021;78(4):1233–1261.
7. Ren Y, Ichinose T, He M, et al. Co-exposure to lipopolysaccharide and desert dust causes exacerbation of ovalbumin-induced allergic lung inflammation in mice via TLR4/MyD88-dependent and -independent pathways. *Allergy Asthma Clin Immunol*. 2019;15:82. doi:10.1186/s13223-019-0396-4
8. Xu D, Zhao M, Song Y, et al. Novel insights in preventing Gram-negative bacterial infection in cirrhotic patients: review on the effects of GM-CSF in maintaining homeostasis of the immune system. *Hepatol Internat*. 2015;9(1):28–34. doi:10.1007/s12072-014-9588-7
9. Firmal P, K SV, Chattopadhyay S. Insight into TLR4-mediated immunomodulation in normal pregnancy and related disorders. *Front Immunol*. 2020;11:807. doi:10.3389/fimmu.2020.00807
10. Liang W, Huang X, Chen W. The effects of BAI and Baicalein on cerebral ischemia: a review. *Aging Disease*. 2017;8(6):850–867. doi:10.14336/AD.2017.0829
11. J KY, J KH, Y LJ, et al. Anti-inflammatory effect of baicalein on polyinosinic¯polycytidylic acid-induced RAW 264.7 mouse macrophages. *Viruses*. 2018;10(5).
12. Jang H, Lee J, Park S, et al. Baicalein mitigates radiation-induced enteritis by improving endothelial dysfunction. *Front Pharmacol*. 2019;10:892. doi:10.3389/fphar.2019.00892
13. Chen J, Ren Z, Sun X, et al. Baicalein inhibited amino-modified polystyrene nanoplastics induced human umbilical vein endothelial cells pyroptosis by reducing the expression of NLRP3/caspase-1/gasdermin D pathway-related proteins. *Chem Biodivers*. 2025;22:e202500085. doi:10.1002/cbdv.202500085
14. M WS, Xia Y. Baicalein modulates endoplasmic reticulum stress by activating SIRT3 to attenuate the dysfunction of retinal microvascular endothelial cells under high glucose conditions. *Exp Eye Res*. 2025;254:110250. doi:10.1016/j.exer.2025.110250
15. Liang S, Wu Y, Zhang R, et al. TNFSF9 silence impedes cerebral ischemia-reperfusion injury via modulating SLC3A2 EXPRESSION in brain microvascular endothelial cells. *J Molecular Neurosci*. 2025;75(1):12. doi:10.1007/s12031-025-02310-1
16. A SDLAR, Gilsanz F, Maseda E. Epidemiologic trends of sepsis in western countries. *Ann Translat Med*. 2016;4(17):325. doi:10.21037/atm.2016.08.59
17. E RK, C JS, M AK, et al. Global, regional, and national sepsis incidence and mortality, 1990-2017: analysis for the global burden of disease study. *Lancet*. 2020;395(10219):200–211. doi:10.1016/S0140-6736(19)32989-7
18. Tang F, L ZX, Y XL, et al. Endothelial dysfunction: pathophysiology and therapeutic targets for sepsis-induced multiple organ dysfunction syndrome. *Biomed Pharmacothe*. 2024;178:117180. doi:10.1016/j.biopha.2024.117180
19. Guo X, Zhang M, Li Q, et al. Evaluation of genetic variants in MIR3142HG in susceptibility to and prognosis of glioma. *Ame J Clin Oncol*. 2020;43(1):1–8. doi:10.1097/COC.0000000000000587
20. Gao Y, Li S, Dong R, et al. Long noncoding RNA MIR3142HG accelerates lipopolysaccharide-induced acute lung injury via miR-95-5p/JAK2 axis. *Human Cell*. 2022;35(3):856–870. doi:10.1007/s13577-022-00687-4
21. Gong X, Zhu L, Liu J, et al. MIR3142HG promotes lipopolysaccharide-induced acute lung injury by regulating miR-450b-5p/HMGB1 axis. *Mol Cell Biochem*. 2021;476(12):4205–4215. doi:10.1007/s11010-021-04209-y
22. Singh V, Kaur R, Kumari P, et al. ICAM-1 and VCAM-1: gatekeepers in various inflammatory and cardiovascular disorders. *Int J Clin Chem*. 2023;548:117487. doi:10.1016/j.cca.2023.117487
23. Manandhar S, Chambers S, Miller A, et al. Pharmacological inhibition and genetic deletion of cystathionine gamma-lyase in mice protects against organ injury in sepsis: a key role of adhesion molecules on endothelial cells. *Int J Mol Sci*. 2023;24(17):13650. doi:10.3390/ijms241713650
24. Sumagin R, Lomakina E, H SI. Leukocyte-endothelial cell interactions are linked to vascular permeability via ICAM-1-mediated signaling. *Am J Physiol Heart Circulatory Physiol*. 2008;295(3):H969–h77. doi:10.1152/ajpheart.00400.2008
25. K MS, M SI, A CJ. Use of integrative epigenetic and cytogenetic analyses to identify novel tumor-suppressor genes in malignant melanoma. *Melanoma Res*. 2011;21(4):298–307. doi:10.1097/CMR.0b013e328344a003
26. S SHINS, H SJ, Hwang B, et al. Angiopoietin-like protein 4 potentiates DATS-induced inhibition of proliferation, migration, and invasion of bladder cancer EJ cells; involvement of G(2)/M-phase cell cycle arrest, signaling pathways, and transcription factors-mediated MMP-9 expression. *Food Nutrit Res*. 2017;61(1):1338918. doi:10.1080/16546628.2017.1338918
27. Tian Y, Stamova B, C JG, et al. Y chromosome gene expression in the blood of male patients with ischemic stroke compared with male controls. *Gender Med*. 2012;9(2):68–75.e3. doi:10.1016/j.genm.2012.01.005
28. Joffre J, Hellman J, Ince C, et al. Endothelial responses in sepsis. *Am J Respir Crit Care Med*. 2020;202(3):361–370. doi:10.1164/rccm.201910-1911TR
29. Zhang H, Wang Y, Qu M, et al. Neutrophil, neutrophil extracellular traps and endothelial cell dysfunction in sepsis. *Clin transl med*. 2023;13(1):e1170. doi:10.1002/ctm2.1170
30. Barkaway A, Rolas L, Joulia R, et al. Age-related changes in the local milieu of inflamed tissues cause aberrant neutrophil trafficking and subsequent remote organ damage. *Immunity*. 2021;54(7):1494–510.e7. doi:10.1016/j.immuni.2021.04.025
31. Aldabbous L, Abdul-Salam V, Mckinnon T, et al. Neutrophil extracellular traps promote angiogenesis: evidence from vascular pathology in pulmonary hypertension. *Arteriosclerosis Thrombosis Vasc Biol*. 2016;36(10):2078–2087. doi:10.1161/ATVBAHA.116.307634
32. Kolaczkowska E, Kubes P. Neutrophil recruitment and function in health and inflammation. *Nat Rev Immunol*. 2013;13(3):159–175. doi:10.1038/nri3399
33. He H, Zhang W, Jiang L, et al. Endothelial cell dysfunction due to molecules secreted by macrophages in sepsis. *Biomolecules*. 2024;14(8):980. doi:10.3390/biom14080980
34. Zoulikha M, Xiao Q, F BG, et al. Pulmonary delivery of siRNA against acute lung injury/acute respiratory distress syndrome. *Acta pharmaceutica Sinica B*. 2022;12(2):600–620. doi:10.1016/j.apsb.2021.08.009

35. Qiao X, Yin J, Zheng Z, et al. Endothelial cell dynamics in sepsis-induced acute lung injury and acute respiratory distress syndrome: pathogenesis and therapeutic implications. *Cell commun signaling*. 2024;22(1):241. doi:10.1186/s12964-024-01620-y
36. He J, Jing D, Zhao S, et al. BAP31 promotes adhesion between endothelial cells and macrophages through the NF-κB signaling pathway in sepsis. *J Inflamm Res*. 2024;17:1267–1279. doi:10.2147/JIR.S448091
37. H BJ, F LP, Trink J, et al. Endoplasmic reticulum stress as a driver and therapeutic target for kidney disease. *Nat Rev Nephrol*. 2025;21(5):299–313. doi:10.1038/s41581-025-00938-1
38. Xu H, Ye X, Steinberg H, et al. Selective blockade of endothelial NF-kappaB pathway differentially affects systemic inflammation and multiple organ dysfunction and injury in septic mice. *J Pathol*. 2010;220(4):490–498. doi:10.1002/path.2666
39. Luo M, Meng J, Yan J, et al. Role of the nucleotide-binding domain-like receptor protein 3 inflammasome in the endothelial dysfunction of early sepsis. *Inflammation*. 2020;43(4):1561–1571. doi:10.1007/s10753-020-01232-x
40. Kobayashi H, Huang J, YE F, et al. Interleukin-32beta propagates vascular inflammation and exacerbates sepsis in a mouse model. *PLoS One*. 2010;5(3):e9458. doi:10.1371/journal.pone.0009458
41. Mamiya A, Kitano H, Kokubun S, et al. Activation peptide of coagulation factor IX regulates endothelial permeability. *Transl Res*. 2016;177:70–84.e5. doi:10.1016/j.trsl.2016.06.006
42. Chen W, Wang Y, Zhou Y, et al. m1 macrophages increase endothelial permeability and enhance p38 phosphorylation via PPAR-γ/CXCL13-CXCR5 in sepsis. *Int Arch Allergy Immunol*. 2022;183(9):997–1006. doi:10.1159/000524272